Time-Spatial Labeling Inversion Pulse (Time-SLIP) MRI for Evaluating Cerebrospinal Fluid Velocity and Visualizing Flow Dynamics in Patients With Chiari Type I Malformation

Tatsushi Inoue, MD, PhD[*‡], Masahiro Joko, MD, PhD[*], Kazuhiro Murayama, MD, PhD[§], Masato Ikedo, MEng[‖], Fumiaki Saito, MSN[¶], Jun Muto, MD, PhD[*], Hiroki Takeda, MD[‡], Shinjiro Kaneko, MD, PhD[‡], Yuichi Hirose, MD, PhD[*]

[*]Department of Neurosurgery, Fujita Health University, Aichi, Japan; [‡]Department of Spine and Spinal Cord Surgery, Fujita Health University, Aichi, Japan; [§]Department of Radiology, Fujita Health University, Aichi, Japan; [‖]Canon Medical Systems Corporation, Otawara, Japan; [¶]Section of Fujita Nurse Practitioner, Fujita Health University, Aichi, Japan

Correspondence: Tatsushi Inoue, MD, PhD, Department of Neurosurgery and Department of Spine and Spinal Cord Surgery, Fujita Health University, 1-98 Dengakugakubo, Kutsukake-cho, Toyoake, Aichi 470-1192, Japan. Email: spine_expert@mac.com

Received, May 13, 2023; **Accepted,** August 13, 2023; **Published Online,** October 13, 2023.

BACKGROUND AND OBJECTIVES: Phase-contrast MRI is unstable and is not widely implemented in the imaging of Chiari malformation type I (CM-I) because of its low signal-to-noise ratio and the need for subsequent additional averaging. Time-spatial labeling inversion pulse MRI (T-SLIP MRI) is an emerging imaging modality with a high signal-to-noise ratio. This study is the first to examine cerebrospinal fluid (CSF) dynamics on the basis of velocity exclusively in patients with CM-I using T-SLIP MRI before and after posterior fossa decompression.

METHODS: Eleven patients with CM-I underwent T-SLIP MRI before and/or after posterior fossa decompression. CSF dynamics were analyzed at 5 points around the craniovertebral junction. T-SLIP measurements included (1) targeted CSF labeling; (2) manual frame-by-frame annotation of the labeled CSF wave; (3) description of CSF flow in terms of wave functions calculated using computation software; and use of this function for (4) calculation of CSF velocity (rostral and caudal peak), total distance traveled by labeled CSF, and mean CSF velocity ($\bar{V}$). Differences between preoperative and postoperative peak velocity (rostral and caudal) and $\bar{V}$ were assessed using paired *t*-test.

RESULTS: Rostral and caudal peaks significantly increased at 2 of the 5 points (40%), whereas $\bar{V}$ significantly increased at 4 points (80%), altogether covering all observation points with significant changes. CSF filling the syrinx through the syrinx wall from the spinal subarachnoid space and complex CSF flow at the dorsal craniovertebral junction were captured preoperatively and postoperatively, respectively.

CONCLUSION: T-SLIP MRI data for patients with CM-I were successfully quantified on the basis of velocity. Tailor-made optimal decompression should be pursued based on both T-SLIP data with high accuracy and bibliographical craniometric data with surgical outcomes, which can now be easily and comprehensively analyzed using machine learning.

KEY WORDS: Cerebrospinal fluid, Chiari malformation type I, Dynamics, MRI, Time-spatial labeling inversion pulse, Velocity, Time-SLIP

Neurosurgery Practice 2023;4(4):e00065. https://doi.org/10.1227/neuprac.0000000000000065

Chiari malformation type I (CM-I) with a syrinx has inspired many surgeons to elucidate the mechanisms underlying syrinx formation. MRI noninvasively evaluates cerebrospinal fluid (CSF) dynamics in patients with CM-I, with phase-contrast (PC) MRI being the most common method. However, PC-MRI data[1-8] are generally unstable (Table 1)[6,9] and are impractical for clinical use.[9] Time-spatial labeling inversion pulse MRI (T-SLIP MRI), developed in 2008,[10] reportedly has the advantages of accurate and moment-by-moment observation of the distribution of labeled CSF. One of its disadvantages, however, is that it is not fit for quantification. This study is the first to quantify T-SLIP MRI data based on CSF flow velocity in patients with CM-I.

ABBREVIATIONS: CM-I, Chiari malformation type I; **CVJ,** craniovertebral junction; **FM,** foramen of Magendie; **PC-MRI,** phase-contrast MRI; **PFD,** posterior fossa decompression; **TI,** inversion time; **T-SLIP MRI,** Time-spatial labeling inversion pulse MRI.

TABLE 1. Literature Review of the MRI-PC CSF Velocity Study

Study (Year)	Control vs CMI	Pre-PFD vs Post-PFD
Delavari (2020)[1]		↗
Nishikawa (2021)[2]	↘	↗
Iskander (2004)[3]		↘[a]
Vinje (2018)[4]		↘
Sakes (2005)[5]	↘	↗
Williams (2021)[c,6]	↗	
Haughton (2003)[7]	↗	
Clarke (2013)[8]	↗[b]	

CM-I, Chiari malformation type I; CSF, cerebrospinal fluid; PC-MRI, phase-contrast MRI; PFD, posterior fossa decompression.
[a]Decreased in 5 cases of total 8 cases (63%).
[b]Caudal direction without syringomyelia.
[c]Meta-analysis composed of 14 studies.
↗ and ↘: increases and decreases in CMI or Post-PFD, respectively.

METHODS

Patient Population

In this retrospective, single-center study, we analyzed the data of 41 pediatric and adult patients with spinal diseases who underwent T-SLIP MRI between November 2014 and March 2021 at our institution. This study was approved by the ethical review board of the Fujita Health University (approval number: HM22-031), who waived the requirement for informed consent, as T-SLIP MRI is usually requested to be performed by Japanese neurosurgeons. Instead, a choice to opt out of this study was announced on the website of the homepage of the Fujita Health University.

CM-I was defined on MRI as cerebellar tonsillar herniation >5 mm below the foramen magnum. Patients with symptomatic CM-I with and without syrinx who had undergone posterior fossa decompression (PFD) were included, whereas patients with non–CM-I–related pathology, including a syrinx without CM-I, sacral cyst, conservatively managed CM-I, and instrumented decompression for CM-I with basilar invagination, were excluded (Figure 1). Routine and T-SLIP MRI evaluations were performed preoperatively and postoperatively.

Surgery

In this series, the posterior fossa was decompressed at the width of the posterior occipital condyle, not exceeding 3 cm.[11] The upper extension of the craniotomy was tailored to restore obstructed CSF dynamics based on the T-SLIP images of the occipital zone, while ensuring that it did not exceed approximately 3 cm. The dura was opened using a Y-shaped incision under a microscope, preserving the arachnoid membrane as much as possible. The patency of the foramen of Magendie (FM) was confirmed preoperatively using T-SLIP in all patients. Duraplasty was performed using Gore-Tex and a non-penetrating microclip (LeMaitre Vascular, Inc) to ensure secure sutures[12] (Figure 2).

Acquisition of T-SLIP MR Images

T-SLIP MR images were acquired using a 3-T MRI system (Vantage Titan 3T; Canon Medical Systems) equipped with a 32-channel head coil (32ch Head SPEEDER; Canon Medical Systems). T-SLIP imaging involves an arterial spin labeling technique that makes it possible to directly and noninvasively visualize CSF flow using MRI, capturing CSF dynamics for 4 to 5 s.[10] First, a spatially free selected inversion pulse is applied in a belt-shaped manner, covering the craniovertebral junction (CVJ), including the foramen magnum, occiput, and C1 vertebra (Figure 1). T-SLIP images are acquired after repeated scanning at different delay times. T-SLIP imaging with a fast advanced spin-echo two-dimensional sequence was performed using the following parameters: repetition time, 10R-R (peripheral gating mode); echo time, 80 ms (echo train spacing, 5.0 ms); matrix, 320 × 320; field of view, 25 × 25 cm; slice thickness, 5.0 mm; flip angle, 90°/160°; number of slices, 1; parallel imaging (SPEEDER; Canon Medical Systems) reduction factor, 2.0; black blood inversion time (TI) prep, on; T-SLIP TI initial value, 2000 ms; T-SLIP TI step, 100 ms; number of repetitions, 30; and T-SLIP pulse thickness, 10.0 mm.

In one patient, supplementary T-SLIP images were obtained at the cervical syrinx level because routine imaging showed a centrifugal CSF cavity particularly close to the subarachnoid space. A spatially free selected inversion pulse, including a thin border between the syrinx and subarachnoid space along the posterior horn, was applied.

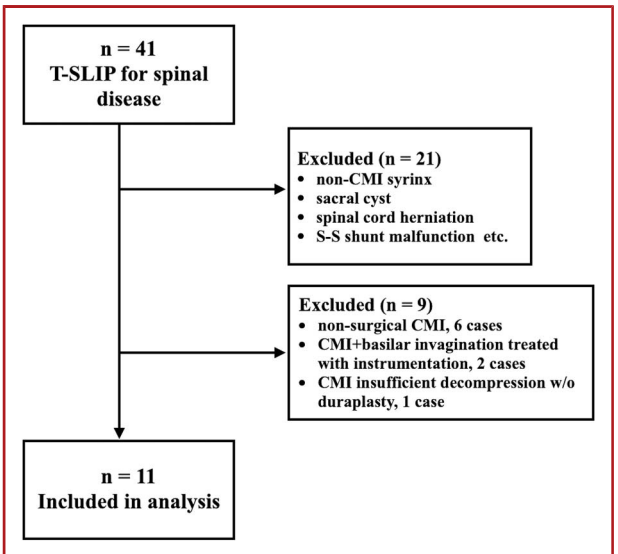

FIGURE 1. *Flowchart of cases based on the study protocol. CM-I, Chiari malformation type I; T-SLIP, time-spatial labeling inversion pulse.*

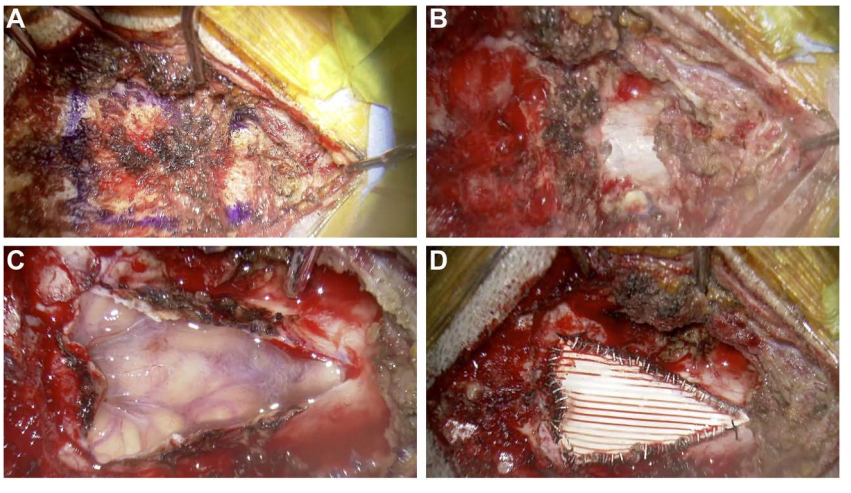

FIGURE 2. *Posterior fossa decompression in this study: Patient 9 is considered representative.* **A**, *First, the occipital bone and C1 lamina are exposed.* **B**, *Subsequently, the occipital bone is removed at the width of the occipital condyle and at the length to restore the balanced cerebrospinal fluid stream between points 4 and 5 on time-spatial labeling inversion pulse MRI, not to exceed approximately 3 cm in both, with C1 laminectomy.* **C**, *Subsequently, the dura is opened in a Y-shaped fashion, keeping the arachnoid membrane intact.* **D**, *Thereafter, duraplasty by Gore-Tex is performed with a nonpenetrating microclip.*

Analysis of CSF Dynamics

Labeled CSF was examined using Osirix MD (Pixmeo SARL, Inc) at the following starting points: point 1, rostral ventral labeled CSF border; point 2, caudal ventral border; point 3, caudal dorsal border; point 4, rostral dorsal border; and point 5, FM (Figure 3). Each labeled CSF border was traced on 28 to 30 frames, which were obtained every 100 ms. The distance (*d*) between the starting point and apex of the most distantly labeled region was measured (Figure 3). Distances measured into the tagged zone were deemed positive (ie, caudal flow was considered positive at points 1, 4, and 5; and cephalad flow was considered positive at points 2 and 3), whereas those measured away from the zone were deemed negative.

The distance was plotted on a distance–time graph, and interpolation and curve fitting were performed. By differentiating the interpolating function on the distance–time curve, the velocity–time function and curve were generated using Mathematica (Wolfram Research, Inc) (Figure 4).

The total distances traveled by CSF in the positive and negative directions were calculated by integrating the velocity–time curve (Figure 5). The total distance traveled by CSF was subsequently divided by the corresponding time (2800-3000 ms) to obtain the mean velocity ($\bar{V}$). The maximum and minimum flow velocities were determined from the velocity–time curve using the FindMinimun and FindMaximum functions in Mathematica.

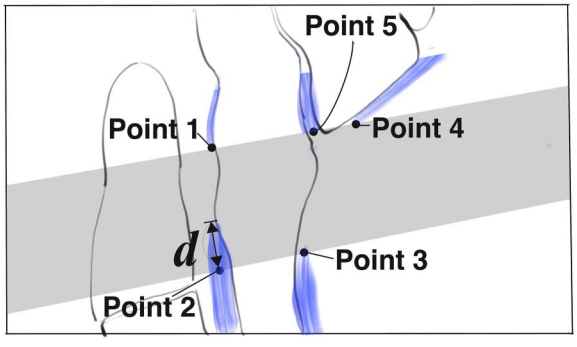

FIGURE 3. *Five measurement points for CSF dynamics via T-SLIP MRI around the craniovertebral junction. The shaded zone represents the CSF area tagged by T-SLIP MRI. The distance between the starting point and apex of the most distantly labeled region was defined as "d." CSF, cerebrospinal fluid; T-SLIP MRI, time-spatial labeling inversion pulse MRI.*

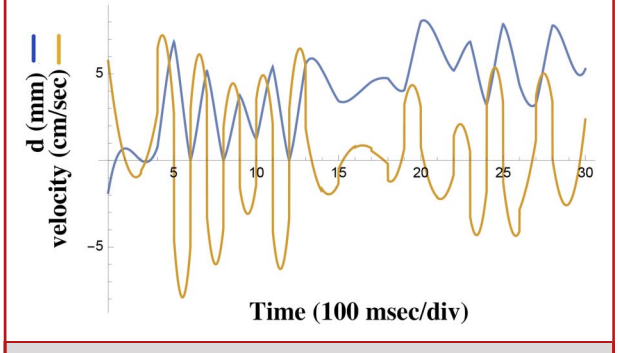

FIGURE 4. *Representative waveform of the time–distance curve (blue) and time–velocity curve (orange). Data are acquired from patient 1 postoperatively.*

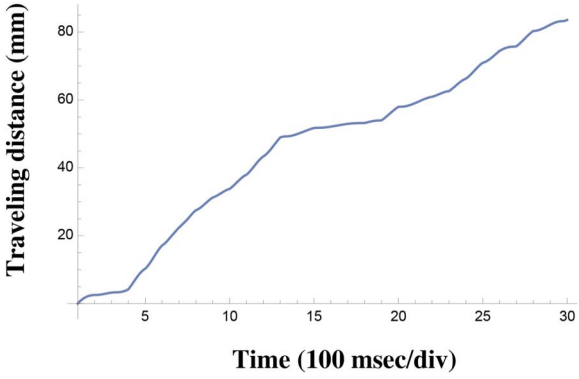

FIGURE 5. *Total distance traveled by cerebrospinal fluid, calculated by integrating the velocity-time curve. Note that the absolute values in both positive and negative directions of velocity are integrated as the "total" distance traveled. The horizontal axis represents the frame number, corresponding to every 100 ms. The vertical axis represents the integrated value of the velocity–time function from frame one to the digit frame. Output is obtained using Mathematica. Data are obtained for case 1 at postoperative point 4.*

Statistical Analysis

Preoperative and postoperative $\bar{V}$ values were compared among points 1 to 5 using the paired *t*-test, following a check of data normality using the Shapiro–Wilk test in SPSS software (v28; IBM Corp). Statistical tests were two-sided, and *P*-values < .05 were considered statistically significant. Our missing data analysis procedures used "missing at random" assumptions. We used multiple imputation methods in SPSS. We independently analyzed 5 copies of the data, each with missing values suitably imputed.

RESULTS

Eleven patients with CM-I (4 men; mean age, 35.4 [range, 12-67] years) were included (Table 2), whereas the remaining 30 patients were excluded (Figure 1). The mean interval between the operation day and postoperative T-SLIP MRI was 26.0 (range, 1-68) months. Eight patients had a syrinx, whereas 3 did not. The postoperative course was satisfactory in all patients, with all 8 patients showing reduced syrinxes (100%). No cases demonstrated infection, CSF leak that needed repair, or new additional neurological signs/symptoms.

Three patients did not have preoperative MR images. In one patient (Patient 10) for whom image acquisition was incorrectly performed, the number of repetitions was correct at 30, although only 15 repetitions were acquired. Hence, preoperative data for this patient were rejected. Two other patients (Patients 9 and 11) missed their MRI examination at our institute and these data were substituted with routine MRI without T-SLIP data, brought from their referring hospital, for preoperative imaging. The type of data defect was estimated to be missing at random.

A summary of CSF velocity measurements is presented in Table 3A. There was no evidence of non-normality among the measurements (Table 3B). Preoperative and postoperative mean $\bar{V}$ values ranged from 0.8 to 2.7 cm/s and 1.6 to 4.8 cm/s, respectively. Significant differences in preoperative and postoperative $\bar{V}$ values were observed at points 1, 3, 4, and 5, whereas the

TABLE 2. Demographic Characteristics of 11 Patients With Chiari Malformation Type I

Patient no.	Age (y)/Sex	Preoperative syrinx	Op	Timing of postoperative TS (mo)	CVJ TS images		Supplementary TS images	F/U (mo)
					Preoperative	Postoperative		
1	39/M	+	PFD	1	+	+	–	81
2	13/F	+	PFD	56	+	+	–	67
3	42/F	+	PFD	2	+	+	-	98
4	30/F	–	PFD	50	+	+	–	62
5	32/F	–	PFD	39	+	+	–	51
6	21/M	+	PFD	2	+	+	–	26
7	56/F	+	PFD	8	+	+	+[a]	32
8	12/M	–	PFD	2	+	+	–	33
9	56/F	+	PFD	11	–	+	–	52
10	21/M	+	PFD	68	–	+	–	144
11	67/F	+	PFD	47	–	+	–	59

CVJ, craniovertebral junction; F/U, follow up; PFD, posterior fossa decompression; TS, time-spatial labeling inversion pulse.
[a]Axial TS image at the cervical syrinx.

TABLE 3A. Summary of Preoperative and Postoperative Peak Rostral and Caudal Velocities

		Preoperative (n = 8)			Postoperative (n = 11)			Preoperative vs Postoperative	
		Max	Min	Mean	Max	Min	Mean	95% CI	*P* value[a]
Rostral peak (cm/s)	Point 1	17.2	1.52	6.81	15.7	4.67	9.55	−6.13 to 0.51	.097
	Point 2	20.9	3.19	10.4	33.2	3.1	13.92	−9.97 to 2.71	.262
	Point 3	8.23	1.09	4.1	13.8	3.13	7.99	−6.49 to −1.51	**.002**
	Point 4	5.79	0.3	2.98	12.2	2.49	6.19	−5.62 to −0.88	**.007**
	Point 5	11	2.16	6.62	14.1	3.58	6.226	−2.79 to 3.28	.876
Caudal peak (cm/s)	Point 1	−1.85	−17.7	−7.47	−4.93	−14.8	−9.83	−1.38 to 6.36	.207
	Point 2	−1	−21.7	−7.92	−1.93	−38.7	−15.77	0.88-14.56	**.027**
	Point 3	−1.58	−10.2	−4.58	−4.59	−9.65	−7.35	−0.13 to 5.65	.061
	Point 4	−0.44	−7.56	−3.04	−1.91	−9.12	−5.46	0.32-4.50	**.023**
	Point 5	−2.08	−10.8	−6.3	−2.61	−13.7	−6.03	−3.41 to 3.15	.938
$\bar{V}$	Point 1	5.19	0.66	2.04	5.8	1.29	3.15	−2.06 to −0.07	**.035**
	Point 2	7.74	0.38	2.54	15.4	1.03	4.83	−4.87 to 0.16	.067
	Point 3	2.53	0.72	1.6	3.25	1.39	2.5	−1.72 to −0.26	**.007**
	Point 4	1.62	0.1	0.85	3.28	0.66	1.8	−1.65 to −0.35	**.002**
	Point 5	7.87	1.02	2.75	2.85	0.83	1.69	0.01-2.46	**.048**

$\bar{V}$, mean cerebrospinal fluid velocity.
Bold values are statistically significant.
[a]Paired-*t* test with multiple imputation for missing values.

rostral peak increased at points 3 and 4, and the caudal peak significantly increased at points 2 and 4.

T-SLIP imaging revealed a "to-and-fro pattern" in CSF dynamics. In the time period from 100 to 2800–3000 ms, the cycles and extremal values of the traveling and velocity waves changed frequently (Figure 4). Moreover, turbulent flow was occasionally observed (Figure 6). T-SLIP stream visualization captured the interactive dynamics of the CSF (Figure 7). Three streams from points 3 (cervical: C), 4 (occipital: O), and 5 (foramen of Magendie: FM) intersected at a point in the posterior CVJ (Figure 7A and 7B). Subsequently, the stream from C pushed the stream from O back when the stream from point FM was blocked by the stream from C (Figure 7C and 7D). Thereafter, the stream from O pushed the stream from C back when the stream from the FM was blocked by the stream from O (Figure 7E and 7F). Subsequently, the stream from the FM pushed the stream from C back when the stream from O was blocked by the stream from the FM (Figure 7G and 7H).

Patient 7 demonstrated an influx of CSF into the syrinx from the subarachnoid space. Preoperative sagittal MR images (Figure 8A and 8B) demonstrated a syrinx in the upper cervical cord (Figure 8A) and in the lower cervical to thoracic cord (Figure 8B), with tonsillar ptosis beyond the foramen magnum. Postoperatively, the syrinx had shrunk with the restoration of the cisterna magna (Figure 8C). The axial image at the C2/3 level (Figure 8D) revealed a syrinx, extending centrifugally and close to the posterior horn and subarachnoid space. The T-SLIP tag was placed in a belt-shaped manner along the posterior horn (Figure 8E). At 1900 ms of delayed time, a faint fan-like CSF inflow was visible, possibly through the thin wall on the cord (Figure 8F and 8G).

DISCUSSION

To the best of our knowledge, this study is the first to use T-SLIP MRI to assess preoperative and postoperative CSF dynamics in patients with CM-I on the velocity base. Compared with PC-MRI, T-SLIP MRI successfully depicted more detailed and sensitive spatial and temporal CSF distribution with quantified dynamics.

In 2018, Ohtonari et al[13] reported the first application of T-SLIP MRI for CM-I to quantify CSF dynamics. The method for quantification was originally defined as quick and simple. In brief, they summated the maximum CSF movement in 2 different directions (rostral and caudal) at 2 different points (ventral and

TABLE 3B. Summary of Normality Checks for Velocity Variables

		Preoperative (n = 8)		Postoperative (n = 11)	
		W	*P* value[a]	W	*P* value[a]
Rostral peak (cm/s)	Point 1	0.828	.056	0.950	.714
	Point 2	0.916	.399	0.883	.199
	Point 3	0.887	.222	0.967	.875
	Point 4	0.960	.807	0.892	.246
	Point 5	0.882	.195	0.844	.083
Caudal peak (cm/s)	Point 1	0.889	.227	0.932	.537
	Point 2	0.879	.183	0.934	.555
	Point 3	0.844	.083	0.098	.075
	Point 4	0.899	.283	0.950	.708
	Point 5	0.866	.139	0.887	.217
$\bar{V}$	Point 1	0.847	.088	0.956	.770
	Point 2	0.829	.058	0.825	.053
	Point 3	0.959	.798	0.966	.863
	Point 4	0.957	.780	0.908	.343
	Point 5	0.824	.051	0.973	.919

$\bar{V}$, mean cerebrospinal fluid velocity.
[a]Shapiro–Wilk test.

dorsal), which were then compared between surgical (preoperative) and nonsurgical groups.[13] The total length of motion (cm) was shorter in the surgical group, meaning that T-SLIP MRI was able to guide surgery.[13] However, in most studies using PC-MRI, the velocity dimension (cm/s) has been used to evaluate CSF dynamics. Therefore, the validity of evaluating CSF dynamics using PC-MRI and T-SLIP MRI was not yet compared in their study.

When using conventional PC-MRI to assess CSF velocity, the peak velocity is retrieved as a property of a wave lasting approximately 1 s. Williams et al[6] conducted a meta-analysis of all studies that quantified CSF velocity, which included healthy controls (n = 91) and Chiari malformation (n = 166) groups. The mean peak velocity at the foramen magnum was 6.4 cm/s on two-dimensional PC-MRI and 8.3 cm/s on four-dimensional PC-MRI. In our study, rostral peak velocity was 3 to 10 cm/s on average, whereas caudal peak velocity was −3 to −8 cm/s on average. Thus, regarding peak velocity, the data from T-SLIP MRI appeared roughly similar to those from PC-MRI reported in the previous meta-analysis.[6]

Herein, we introduced $\bar{V}$ according to T-SLIP MRI. This is obtained from the total traveling distance of the labeled CSF by dividing it by the observation time, which is approximately 3 times longer than in PC-MRI. By introducing $\bar{V}$, we intended to capture the whole CSF wave information besides the peak velocity or maximum movement of tagged CSF. $\bar{V}$ successfully detected postoperative significant changes in CSF dynamics at 4 of the 5 observation points. Although $\bar{V}$ failed to detect CSF dynamics changes at point 2 (P = .067), the caudal peak velocity at point 2 had increased significantly (P = .027). Thus, by combining the newly introduced parameter $\bar{V}$ and the traditional parameter peak velocity, we detected a significant change in the postoperative CSF dynamics, as labeled and traced by T-SLIP MRI, all around the CVJ.

Physical Significance of Mean CSF Velocity ($\bar{V}$)

The CSF wave is a typical irregular wave represented in nature by a wind wave or sea wave where specialized statistics are introduced for analysis using 100 consecutive raw waves.[14] However, such measurement of CSF dynamics cannot be conducted

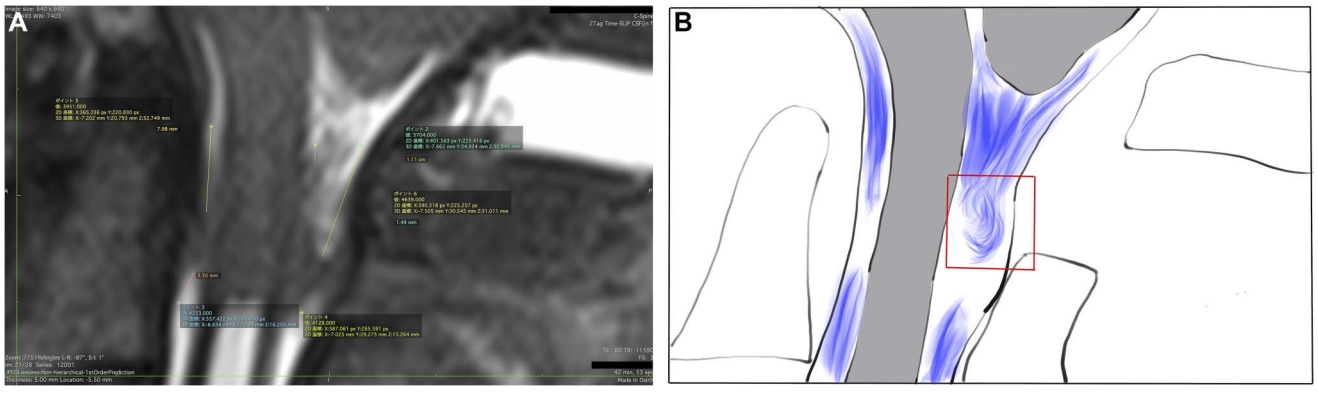

FIGURE 6. *Time-spatial labeling inversion pulse MRI scan for patient 5. Left, postoperative; right, a drawing. Turbulent flow is indicated in the red square on the right-hand figure.*

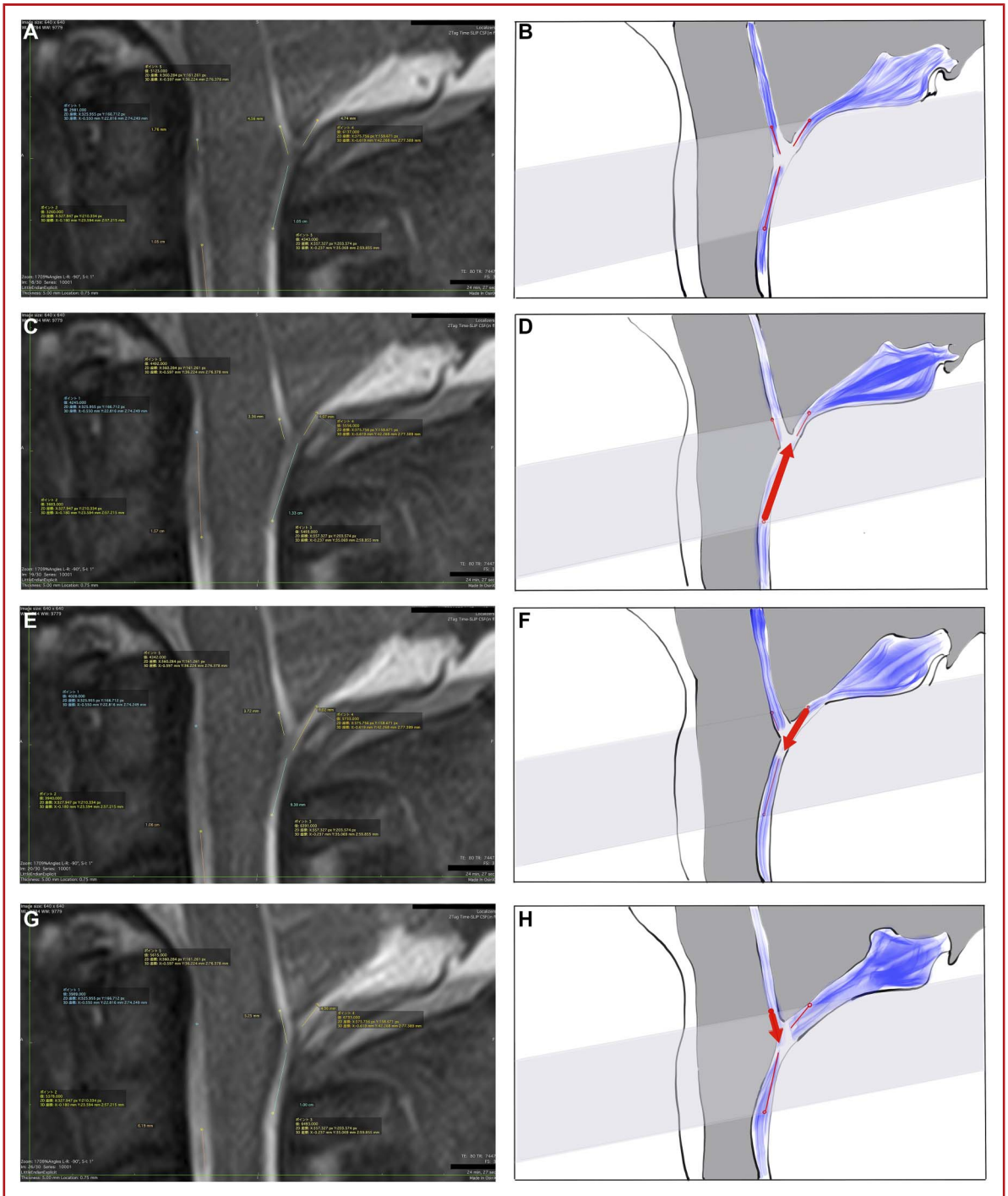

FIGURE 7. *Perspective view of the CSF stream at the posterior CVJ after decompression. Dynamic temporal collision and interference of 3 CSF streams presents with a pattern comparable to that observed in the push-and-shove game.* **A**, *T-SLIP MR image and* **B**, *its corresponding drawing showing 3 streams (red slime lines) intersecting at the posterior CVJ.* **C**, *T-SLIP MR image and* **D**, *its corresponding drawing showing the cervical streams (red arrow) pushing back the occipital stream with the FM stream interrupted.* **E**, *T-SLIP MR image and* **F**, *its corresponding drawing showing the occipital stream (red arrow) pushing back the cervical stream with the FM stream interrupted.* **G**, *T-SLIP MR image and* **H**, *its corresponding drawing showing the FM stream (red arrow) pushing back the cervical stream with the occipital stream interrupted. Data were obtained from patient 1 postoperatively. CSF, cerebrospinal fluid; CVJ, craniovertebral junction; FM, foramen of Magendie; T-SLIP MRI, time-spatial labeling inversion pulse MRI.*

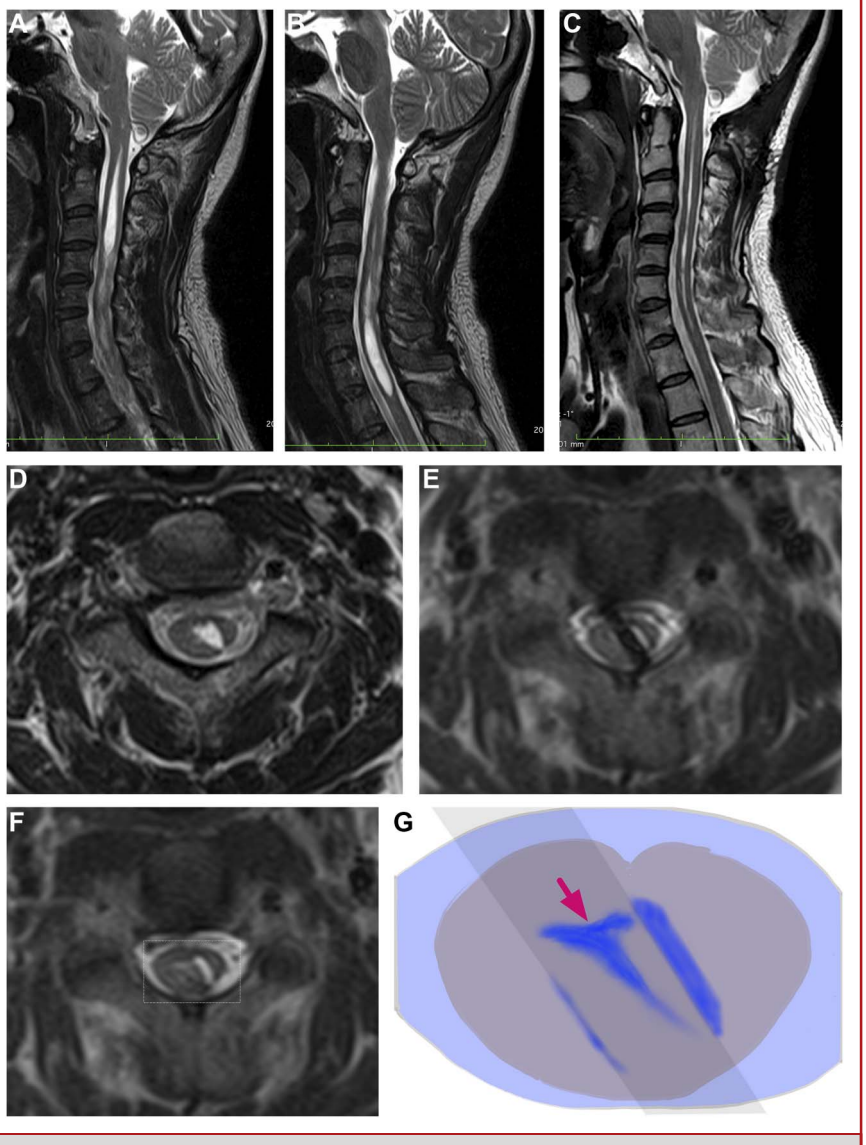

FIGURE 8. *Influx of CSF into the syrinx from the subarachnoid space detected in patient 7.* **A** *and* **B**, *Preoperative sagittal MRI scan demonstrating syrinx* **A**, *in the upper cervical cord and* **B**, *in the lower cervical to thoracic cord* **B**, *with tonsillar ptosis beyond the foramen magnum.* **C**, *Postoperatively, the syrinx is shrunk with the restoration of the cisterna magna.* **D**, *Axial image at the C2/3 level revealing the syrinx, extending centrifugally, close to the posterior horn and subarachnoid space.* **E**, *The tag for time-spatial labeling inversion pulse MRI is placed in a belt-shaped manner along the posterior horn.* **F**, *At 1900 ms of delayed time, a faint fan-like CSF inflow is visible possibly through the thin wall on the cord. Line drawing of the figure* **F**. **G**, *The fan-like CSF is indicated by the arrow. CSF, cerebrospinal fluid.*

noninvasively. In a PC-MRI study, cardiac-gated additionally averaged data were used to introduce a representative value as the peak velocity. In those processes, the effect of respiration is not considered,[15] but not negligible.[15] In this way, there seems to be a limitation in comprehending those values. Iskander et al[3] proposed a novel parameter that better reflects CSF dynamics, after a discussion of that kind of CSF peak velocity data. Although the 3 s of data obtained using T-SLIP are much shorter than 100 consecutive raw waves, which are needed for strict statistical analysis, they were 3 times longer than those obtained using PC-MRI in the present, and we introduced a much more comprehensive parameter, $\bar{V}$, by tracing and measuring the total traveling distance of the point of interest along the entire raw wave. $\bar{V}$ significantly increased postoperatively at 4 of 5 points (points 1, 3, 4,

and 5). However, peak velocity increased at 2 of 5 points (rostral, points 3 and 4; caudal, points 2 and 4). By combining peak velocity data and $\bar{V}$, we were able to detect significant changes after PFD covering the entire CVJ in a point-by-point manner.

Clinical Meaning of the T-SLIP Study

T-SLIP MRI allowed for the detection of changes in CSF dynamics between pre- and post-PFD, covering the entire CVJ. Around the occiput at point 4, all parameters had detected significant postoperative velocity increases, whereas the conventional PC-MRI study had no data on measured velocity because the flow volume was very scant, and setting up the region of interest was difficult. A less-invasive endoscopic decompression with minimized skin incision and bone removal[16,17] is an emerging and promising future research policy, and it is expected to shorten hospital stay and allow for an early return to work/school. Guidelines to decide on the extent of bone removal are essential to avoid insufficient decompression. T-SLIP MRI data would be useful for preoperative essential minimum planning and postoperative evaluation in the future.

Visualization of CSF Inflow Into the Syrinx by T-SLIP: Cue to the Riddle Regarding the Filling Mechanism

Milhorat et al[18] revealed the syrinx cavity as an extension through the dorsal root entry zone to reach the pial surface in an autopsy case with a noncommunicating syrinx. They referred to this as a "rupture" of the syrinx. According to Aboulker's[19] theories, increased pressure drives CSF through the spinal parenchyma or via a pathway along the dorsal root into the spinal cord. In this study, we captured the very moment where the T-SLIP–labeled CSF in the subarachnoid space flowed into the syrinx and diffused. Our findings support Milhorat's[18] findings and Aboulker's[19] theory: the dorsal root and its neighboring area are key for syrinx formation. Myriad theories have been proposed to explain syrinx formation,[20] including classic well-known theories of Gardner,[21] Williams,[22] Ball and Dayan,[23] and Oldfield.[24] In each theory related to syrinx formation, there have been some gaps in explaining the expansion of a syrinx cavity.[20] Currently, using T-SLIP MRI, we partially investigated these important historical questions on the mechanisms of syrinx formation. On T-SLIP MRI, there was no bulk flow forced from the spine to the cisterna magna or no flow into the fourth ventricle and then into the syrinx as in Williams' theory, although Valsalva maneuvers were not performed. Instead, T-SLIP was able to detect a possible inflow from the subarachnoid space around the posterior horn of the cord into the syrinx (Figure 8E), which supports the transmedullary bulk flow theory supported by Milhorat's[25] experimental study rather than the pressure dissociation hypothesis.

Limitations

This study had certain limitations. First, the number of patients (n = 11) was relatively small. We intend to address this in future studies by recruiting more patients. Second, there was a lack of PC-MRI data in CM-I, which precluded quantitative comparisons between PC-MRI and T-SLIP MRI findings. Third, the intervals between preoperative and postoperative MRI varied (2-68 [mean, 26.0] months), which is primarily because we supposed that CSF dynamics would be stable 2 to 3 years postoperatively as the wound hematoma or leaked CSF would have been absorbed, and the syrinx, if it existed, would have shrunk. Conversely, we presumed the process of syrinx formation to be analogous to the reverse of the process of syrinx shrinkage. Therefore, we intended to follow the process of syrinx shrinkage serially using T-SLIP MRI, although the number of included patients (n = 11) was small. As this was a pilot study, further studies using a carefully planned T-SLIP MRI protocol based on these preliminary results are warranted.

CONCLUSION

T-SLIP MRI observations can provide insights into CSF dynamics, which are superior to those provided by PC-MRI and could help elucidate the mechanisms behind syrinx formation. To the best of our knowledge, this study is the first to measure CSF velocity in patients with CM-I using T-SLIP MRI.

Funding

This study did not receive any funding or financial support.

Disclosures

The authors have no personal, financial, or institutional interest in any of the drugs, materials, or devices described in this article. Kazuhiro Murayama received grant funding from Canon Medical Systems Corporation.

REFERENCES

1. Delavari N, Wang AC, Bapuraj JR, et al. Intraoperative phase contrast MRI analysis of cerebrospinal fluid velocities during posterior fossa decompression for Chiari I malformation. *J Magn Reson Imaging.* 2020;51(5):1463-1470.
2. Nishikawa M, Bolognese P, Naitoh K, et al. Outcome of surgical management for syringomyelia associated with Chiari malformation type I□Deciding surgical procedures based on evaluation of cerebrospinal fluid flow at the foramen magnum□. *Spinal Surg.* 2021;35(3):294-303.
3. Iskandar BJ, Quigley M, Haughton VM. Foramen magnum cerebrospinal fluid flow characteristics in children with Chiari I malformation before and after craniocervical decompression. *J Neurosurg.* 2004;101(2 suppl):169-178.
4. Vinje V, Brucker J, Rognes ME, Mardal KA, Haughton V. Fluid dynamics in syringomyelia cavities: effects of heart rate, CSF velocity, CSF velocity waveform and craniovertebral decompression. *Neuroradiol J.* 2018;31(5):482-489.
5. Sakas DE, Korfias SI, Wayte SC, et al. Chiari malformation: CSF flow dynamics in the craniocervical junction and syrinx. *Acta Neurochir (Wien).* 2005;147(12):1223-1233.
6. Williams G, Thyagaraj S, Fu A, et al. In vitro evaluation of cerebrospinal fluid velocity measurement in type I Chiari malformation: repeatability, reproducibility, and agreement using 2D phase contrast and 4D flow MRI. *Fluids Barriers CNS.* 2021;18(1):12.
7. Haughton VM, Korosec FR, Medow JE, Dolar MT, Iskandar BJ. Peak systolic and diastolic CSF velocity in the foramen magnum in adult patients with Chiari I malformations and in normal control participants. *AJNR Am J Neuroradiol.* 2003;24(2):169-176.

8. Clarke EC, Stoodley MA, Bilston LE. Changes in temporal flow characteristics of CSF in Chiari malformation Type I with and without syringomyelia: implications for theory of syrinx development. *J Neurosurg.* 2013;118(5):1135-1140.
9. Greenberg MS. *Handbook of Neurosurgery*. 8th ed. Thieme Medical Publishers; 2016.
10. Yamada S, Miyazaki M, Kanazawa H, et al. Visualization of cerebrospinal fluid movement with spin labeling at MR imaging: preliminary results in normal and pathophysiologic conditions. *Radiology.* 2008;249(2):644-652.
11. Klekamp J, Samii M. *Syringomyelia*. Springer; 2002.
12. Ito K, Aoyama T, Horiuchi T, Hongo K. Utility of nonpenetrating titanium clips for dural closure during spinal surgery to prevent postoperative cerebrospinal fluid leakage. *J Neurosurg Spine.* 2015;23(6):812-819.
13. Ohtonari T, Nishihara N, Ota S, Tanaka A. Novel assessment of cerebrospinal fluid dynamics by time-spatial labeling inversion pulse magnetic resonance imaging in patients with Chiari malformation type I. *World Neurosurg.* 2018; 112:e165-e171.
14. Goda Y. Statistical properties and spectra of sea waves. In: *Random Seas And Design of Maritime Structures*, Vol 33. 3rd edWorld Scientific; 2010:19-61.
15. Yamada S, Miyazaki M, Yamashita Y, et al. Influence of respiration on cerebrospinal fluid movement using magnetic resonance spin labeling. *Fluids Barriers CNS.* 2013;10(1):36.
16. Di X. Endoscopic suboccipital decompression on pediatric Chiari type I. *Minim Invasive Neurosurg.* 2009;52(3):119-125.
17. Ratre S, Yadav N, Parihar V, Bajaj J, Kher Y, Yadav Y. Endoscopic management of Arnold-Chiari malformation type I with or without syringomyelia. *J Neurol Surg A Cent Eur Neurosurg.* 2018;79(1):45-51.
18. Milhorat TH, Capocelli AL, Jr., Anzil AP, Kotzen RM, Milhorat RH. Pathological basis of spinal cord cavitation in syringomyelia: analysis of 105 autopsy cases. *J Neurosurg.* 1995;82(5):802-812.
19. Aboulker J. Syringomyelia and intra-rachidian fluids. IX. The rachidian fluid: its relations with the spinal cord, its place in CSF, its movements. *Neurochirurgie.* 1979;25(suppl 1):81-97.
20. Stoodley M. The filling mechanism. In: Flint G Rusbridge C, editors. *Syringomyelia*. Springer; 2014:87-101.
21. Gardner WJ, Abdullah AF, McCormack LJ. The varying expressions of embryonal atresia of the fourth ventricle in adults: Arnold-Chiari malformation, Dandy-Walker syndrome, arachnoid cyst of the cerebellum, and syringomyelia. *J Neurosurg.* 1957;14(6):591-607.
22. Williams B. The distending force in the production of communicating syringomyelia. *Lancet.* 1970;296(7662):41-42.
23. Ball MJ, Dayan AD. Pathogenesis of syringomyelia. *Lancet.* 1972;300(7781):799-801.
24. Oldfield EH, Muraszko K, Shawker TH, Patronas NJ. Pathophysiology of syringomyelia associated with Chiari I malformation of the cerebellar tonsils. Implications for diagnosis and treatment. *J Neurosurg.* 1994;80(1):3-15.
25. Milhorat TH, Fox A, Todor DR. Pathology, classification, and treatment of syringomyelia. In: Tamaki N, Batzdorf U, Nagashina T, editors. *Syringomyelia*. Springer; 2001:10-30.

Acknowledgments

The coauthor, Masato Ikedo, is a Master of Engineering (MEng).The coauthor, Fumiaki Saito, is a Master of Science in Nursing (MSN).

COMMENTS

Thank you so much for your information. I am very interested in this article. This article described the application of time-spatial labeling inversion pulse MRI (T-SLIP MRI) to the examination CSF dynamics. This new strategy makes it possible to examine pure and single-stroke CSF movement. Also, the authors compared T-SLIP MRI between preoperative and postoperative in Chiari malformation. They discussed CSF flow dynamics at foramen magnum levels in pure Chiari malformation based on the results. This challenge by the authors let the examination of the CSF dynamics develop more. I think that this T-SLIP MRI may be a breakthrough to the study of CSF flow dynamics. Although I think that the discussion of the author is logical, based on the results from a few cases, there may be many objections. But I am able to understand the idea of the author as one hypothesis about CSF dynamics at the foramen magnum. This study is limited by a very small sample size, especially considering 3 of the 11 patients did not have a preoperative MRI, and the authors recognize this in the limitations and state that this is a pilot study. I strongly encourage the authors to continue this study, with normal controls (volunteers) and more cases.

Misao Nishikawa, MD, PhD
Osaka, Japan